論文の内容の要旨

Mapping the Universe with Weak Lensing from Subaru Hyper Suprime-Cam Survey

(すばるハイパースープリムカムサーベイ観測による重力レンズマップ生成)

Xiangchong Li (李翔翀)

The ΛCDM model (also known as concordance cosmology), which is the current standard cosmology model, provides a simple but reasonably good explanation of the observations on the large-scale structure of the Universe. In this model, the Universe is dominated by dark energy (Λ) and cold dark matter (CDM). To be more specific, roughly 68% of the Universe is dark energy, 27% is dark matter, and less than 5% is normal matter. Both dark energy and dark matter behave substantially differently from normal matter: Dark energy has a negative pressure that can cause cosmological expansion; Dark matter only feels the force of gravity, whereas it does not interact electromagnetically. Even though dark matter distribution is traced by galaxy distribution in the Universe, which can be directly observed by telescopes, the relation between the observed galaxy distribution and the properties of the underlying dark matter distribution has not been precisely understood.

Weak gravitational lensing, a phenomenon of light from distant source galaxies being bent by the foreground density fluctuation due to gravity, results in weak but coherent shear distortions on background galaxy images, which anisotropically stretches galaxy shapes (for review, see Bartelmann & Schneider, 2001). Weak lensing hence offers a probe into the foreground inhomogeneous mass distribution by measuring the coherent shear distortion from background galaxies. Since weak lensing is purely caused by the gravitational effect, it is sensitive to not only normal matter (e.g., galaxies, galaxy clusters, intergalactic gas) but also dark

matter. Using measurements of lensing shear distortions from a large ensemble of galaxy images across large areas of the sky, it is possible to directly reconstruct three dimensional (3D) mass maps that are majorly composed of the dark matter without relying on the knowledge of the connection between normal matter and dark matter. The ΛCDM model and weak gravitational lensing are reviewed in Chapter 1.

The Subaru Hyper Suprime-Cam (HSC; Aihara et al., 2018a) survey, which is an optical galaxy image survey, target to recording galaxies over ~ 1400 deg^2 with optical depth reaching ~ 26th magnitude in its i-band filter. By measuring the background galaxy shapes record by the HSC survey, it is possible to map the matter distribution of the Universe and understand the evolution of the large-scale structure over a wide range of redshift.

However, there are two difficulties in 3D weak lensing mass map reconstructions: (i) Weak lensing shear distortion is only about 10% of galaxy's intrinsic shape dispersion and shape measurement error due to photon noise. Controlling the systematics in the measurements (e.g., from point-spread function, noise, and selection) of such small signals is challenging. (ii) The weak lensing shear distortion on a source galaxy is proportional to the integral of structures along the line-of-sight from the observer to the source galaxy. It is challenging to derive a high-resolution mass map from integrated mass maps observed at a few source galaxy redshifts. That is, it is difficult to avoid smearing of structures along the line-of-sight.

This thesis presents the three-year HSC shear catalog that will be used for HSC weak lensing science and reconstructs 3D weak lensing mass maps using the three-year HSC shear catalog. The structure of the thesis is demonstrated in Figure 1 and summarized as follows:

(i) I present the three-year HSC shear catalog that will be used for HSC weak lensing science in Chapter 2 following Li et al. (2021b). I construct realistic galaxy image simulations that can be used to test and calibrate the estimations of weak lensing shear distortions. The image simulations transform high-resolution, high-SNR galaxy images from the Hubble space telescope (Leauthaud et al., 2007) in the COSMOS region to the HSC-like images (Mandelbaum et al., 2018a) according to the observational condition of the HSC (e.g., noise and point-spread function). With a 24.5th magnitude cut, the number histograms over galaxy properties (including size, brightness, shape) of the simulated galaxies match those of the real HSC galaxies; that is, the difference between the simulation and observation is less than 1%. This galaxy image simulation is used to calibrate weak lensing measurement and produce galaxy shape catalogs.

(ii) I develop the FPFS estimator for weak lensing shear distortions with minimal dependence on calibrations from image simulations in Chapter 3 following Li et al. (2018); Li et al. (2020). The estimator uses four polar shapelet modes (Massey & Refregier, 2005) that are calculated from the power function of

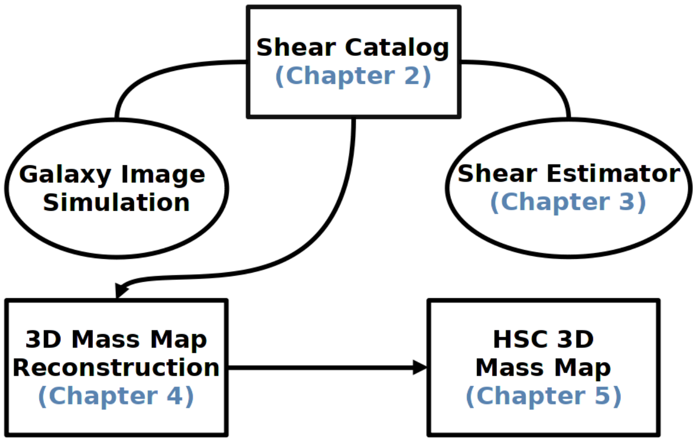

FIGURE 1: Outline of the dissertation.

the Fourier transforms of galaxies after deconvolving the point-spread functions in Fourier space (Zhang & Komatsu, 2011) after deconvolving the PSF's power function. The FPFS estimator is able to recovery weak lensing shear distortion with sub-percent level accuracy for isolated galaxies. However, unfortunately, it requires calibrations for a $\sim 5\%$ shear estimation bias under the conditions that blending exist.

(iii) I develop a sparsity-based mass map reconstruction algorithm for high-resolution 3D mass map reconstructions in Chapter 4 following Li et al. (2021a). The primary difficulty in the 3D mass map reconstruction is that the lensing kernels for lens systems at different redshifts are highly correlated. As a result, the standard lasso sparsity algorithm, which uses the l^1 penalty for model selection and estimation, can not tell in which lens redshift bin the mass is located. Therefore, the mass maps reconstructed with the l^1 lasso algorithm suffer from smears of the structure along the line of sight. Therefore, the mass maps reconstructed with the l^1 lasso algorithm suffer from smears of the structure along the line of sight. The adaptive lasso is a derivative version of the lasso algorithm which applies adaptive weights to penalize different parameters. By using the adaptive lasso algorithm, the smears of the structure along the line of sight are eliminated since the adaptive lasso algorithm is an approximation of l^0 penalty, which prefers a sparser solution, and it is able to select the related models consistently regardless of the correlations between models Zou (2006). I propose to represent the clumpy density distribution as a summation of Navarro-Frenk-White halos (Navarro et al., 1997) with different scales in comoving coordinates to improve the line-of-sight resolution. The algorithm is able to detect halo with minimal mass limits of $10^{13.5} M_\odot/h$, $10^{14.3} M_\odot/h$, $10^{15.0} M_\odot/h$ for the low ($z < 0.3$), median ($0.3 \leq z < 0.6$) and high ($0.6 \leq z < 0.9$) redshifts, respectively. The redshifts estimated by the algorithm is slightly lower than the true redshift by 0.03 for halos with input redshifts ranging from 0.1 to 0.4. For halos at other redshifts, no obvious bias in redshift estimation is found.

(iv) I reconstruct 3D weak lensing mass maps using the weak lensing shear distortions measured from HSC galaxies (Li et al., 2021b) in Chapter 5. Galaxy clusters (groups), the most massive bounded objects in the Universe, are identified from the reconstructed 3D mass maps. In addition, the mass map provides redshift and mass information of the identified galaxy clusters (groups). The galaxy clusters (groups) detected from weak lensing 3D mass maps are matched to cluster catalogs detected from the distributions of galaxies for cross-comparison.